PHILOSOPHICAL MAGAZINE A, 1991, VOL. 64, NO. 1, 87–96

High-resolution transmission electron microscopy study of gold particles (greater than 1 nm), epitaxially grown on clean MgO microcubes

By S. GIORGIO, C. CHAPON, C. R. HENRY

Centre de Recherche sur les Mécanismes de la Croissance Cristalline, Laboratoire Propre du CNRS associé aux Universitiés d'Aix-Marseille 2 et 3, Campus de Luminy, Case 913, 13288 Marseille Cédex 9, France

G. NIHOUL

Groupe de Microscopic Electronique de Toulon, Université de Toulon, B.P.132, 83957 La Garde Cedex, France

and J. M. PENISSON

Departement de Recherche Fondamentale, Service de Physique, Groupe Structures, Centre d'Etudes Nucléaires de Grenoble 85X, 38041 Grenoble Cedex, France

[*Received 31 May 1990 and accepted 19 September 1990*]

ABSTRACT

Gold particles (greater than 1 nm) were vacuum deposited on clean surfaces of MgO microcubes *in situ* synthesized in a controlled atmosphere. The particles were observed simultaneously with the MgO substrate in plan view and in cross-section by high-resolution transmission electron microscopy, microdiffraction and convergent-beam electron diffraction. The gold particles (less than 4 nm) had a f.c.c. structure and were perfectly accommodated with the substrate, leading to a lattice expansion of 2·9%. In this size range (1–4 nm), all the particles were single crystals and had an half-octahedron shape with (001) truncations on the edges. The interface between the particles and the MgO substrate was flat; no defects were imaged. In contrast larger (greater than 4 nm) particles have the lattice parameter of the bulk material. The high stability of the particles in the electron beam was certainly due to their strong interaction with the clean MgO surface.

§ 1. INTRODUCTION

Small (less than 5 nm) metallic particles are interesting from a fundamental point of view in being neither molecular nor bulk material. Variations in the physical and chemical properties have been observed as the size of the particles decreases. For example, their melting point is lowered (Kofman, Cheyssac and Garrigos 1990), and their lattice spacing can change (Balerna *et al.* 1985, Heinemann and Poppa 1985). Furthermore, a non-bulk structure with five-fold symmetry (icosahedron and decahedron) has been observed (Ino 1966, Gillet 1977, Marks and Smith 1983, Giorgio, Urban and Kunath 1989). Such particles are in fact multiply twinned, a low twin-boundary energy and the low surface energy of the (111) facets ensuring their stability (at least for gold and silver) (Ino 1969, Howie and Marks 1984, Marks 1984). Recent high-resolution transmission electron microscopy (HRTEM) investigations have shown that small particles (1–4 nm) undergo rapid structural transitions between f.c.c. single crystals and multiply twinned particles (MTPs) (Iijima 1987). These structure fluctuations were mainly due to the high imaging current used in HRTEM (10–100 A cm^{-2}). However, a careful study by ultra-high-vacuum HRTEM using a low

electron beam intensity has proved that gold particles 2–3 nm in diameter can exhibit stable MTP structures at room temperature. Only particles of 1 nm or less undergo structural fluctuations at room temperature (Mitome, Tanishiro and Takayanagi 1989). These observations are in agreement with calculations of Marks and co-workers (Ajayan and Marks 1988, Dundurs, Marks and Ajayan 1988), indicating that particles smaller than 2 nm are in a 'quasi-molten' state at room temperature. That means that the energy barrier between different particle shapes (cuboctahedron, decahedron or icosahedron MTPs) is of the order of kT, where the temperature T is far below the bulk melting point. From previous observations, MTPs only appear in the gas phase (Hall, Flüeli, Monot and Borel 1989) or on weak interactive or contaminated substrates. In contrast, on clean single-crystalline substrates, metallic particles grow (generally in epitaxy with the substrate) with the bulk structure (Kern, Lelay and Metois 1979, Honjo and Yagi 1980). The crucial role played by the substrate has been recently confirmed by HRTEM by Ajayan and Marks (1989). They showed that some gold particles grown on MgO microcubes could be either unstable (quasi-melting activated by the electron beam heating) or stable (f.c.c. structure), depending on their interaction with the substrate. During strong beam exposure, the particle–substrate interface evolves; then the particle becomes less bonded to the substrate and reaches the quasi-molten state.

The present paper reports the structure, morphology and stability of 1–4 nm gold clusters epitaxially deposited on clean surfaces of MgO microcubes and coated with a thin carbon film to avoid contamination during the ex situ transmission electron microscopy (TEM) observations. These 1–4 nm clusters are compared with larger particles produced in the same experimental conditions.

MgO microcubes have often been used as supports for particles to allow both top and profile views of the particles (Cowley and Kang 1983, Cowley and Neumann 1984, Datye and Long 1988, Marks, Hung, Zhang and Teo 1988, Ajayan and Marks 1989, Giogio, Henry, Chapon and Penisson 1990) but in all these experiments the MgO was exposed to air and therefore contaminated (Duriez, Chapon, Henry and Rickard 1990). However, as we are aware of the dramatic effect of water vapour exposure of MgO surface for subsequent particle growth, we have developed in a previous study a vacuum deposition technique for metal onto clean MgO cubes prepared *in situ* in the evaporation chamber (Giorgio *et al.* 1990).

§2. Epitaxial growth of gold on MgO

2.1. *Sample preparation*

A magnesium ribbon was burnt in a mixture of pure oxygen (20%) an nitrogen (80%), at a total pressure of 10^5 Pa in the vacuum chamber; the MgO cubes were collected on a molybdenum microscope grid coated with a carbon film and heated at 150°C to prevent contamination by a residual H_2O trace concentration while evacuating the chamber. When the pressure reached 1×10^{-6} Pa, the microscope grid was brought in front of a Knudsen cell for the gold evaporation at a rate of 1×10^{13} atoms $cm^2 s^{-1}$. During the deposition (2–4 min), the pressure increased to 1×10^{-5} Pa. Before removal of the sample, a thin carbon film was deposited on the sample both to avoid further contamination and to prevent charging effects during subsequent observation in the electron microscope. Indeed, artefacts produced by charging have often been noticed in the high-resolution images of MgO cubes (Tanji *et al.* 1989).

2.2 *Observations in conventional TEM*

The samples were first observed in a JEOL 2000FX operating at 200 kV. Figure 1 (*a*) shows a typical image of MgO cubes covered with gold particles (2–4 nm). The gold particles grown on the carbon film are smaller and more numerous than on MgO because of the higher nucleation rate on the former substrate, and their structures (fig. 1 (*b*)) are often multiple twins.

Fig. 1

(*a*)

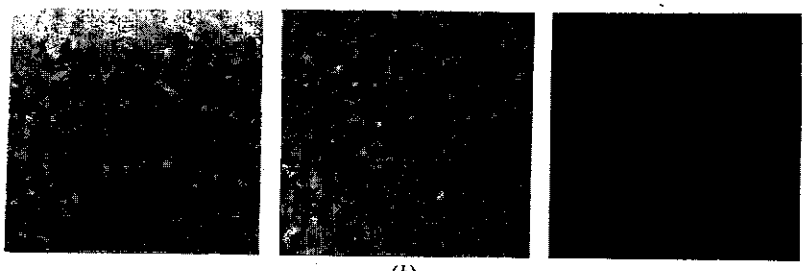

(*b*)

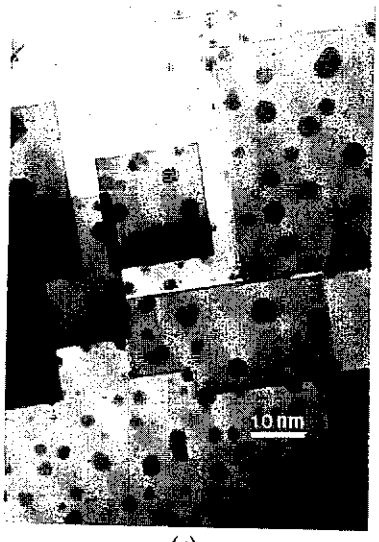

(*c*)

(*a*) Overview of gold particles sitting on the surfaces and edges of MgO cubes. (*b*) Particles with five-fold symmetries, lying on the carbon film. (*c*) Large (greater 4 nm) gold particles on the surface of MgO cubes.

In most of the previous works on MgO smoke, the MgO surfaces exhibited a high density of defects (steps and kinks). In contrast, for MgO cubes prepared under the clean conditions described here, no defects are visible on the MgO surfaces.

The f.c.c. structure of individual particles was verified using selected-area diffraction (SAD) in low-convergence illumination, with an electron beam diameter reduced to 20 nm at the sample and convergent-beam electron diffraction (CBED) with a 4 nm sampling diameter. The epitaxial relationships were determined by micro-diffraction. The diffraction patterns (fig. 2(*a*)) do not show any splitting of the diffraction spots, indicating that gold particles grow with the lattice relation $(001)_{Au}$ and $\langle 001\rangle_{Au} \| (001)_{MgO}$ and $\langle 001\rangle_{MgO}$ and that they have the same lattice spacing as MgO to $\pm 0{\cdot}5\%$, which is the precision of the measurements. Let us recall that for palladium particles, about 3 nm in size, we could see the splitting of microdiffraction spots (Giorgio *et al.* 1990) although palladium diffracts with lower intensity than gold.

Fig. 2

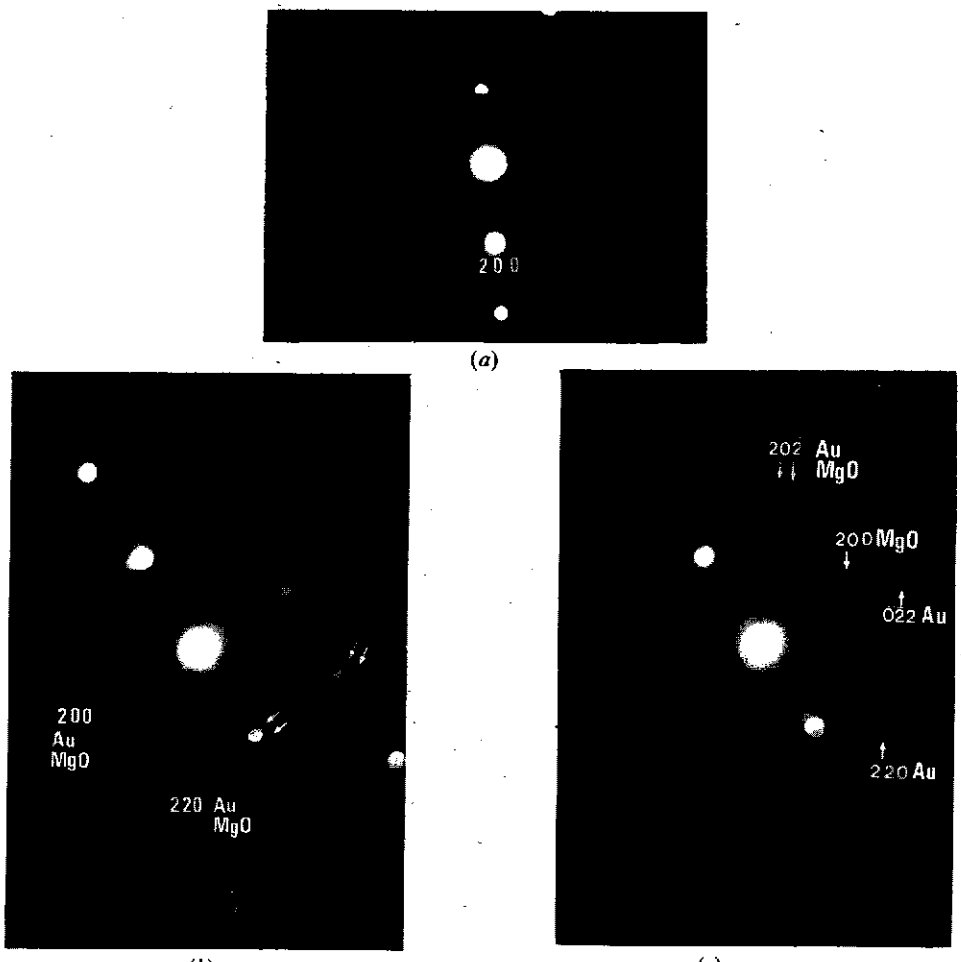

(*a*) SAD pattern of two isolated small particles epitaxially grown on MgO, selected with an electron beam diameter of 20 nm on the edge of a cube. (*b*) SAD of an isolated large particle on MgO in the (100) epitaxial orientation. The 200 reflections are split. (*c*) SAD of a large particle in the (111) epitaxial orientation on MgO.

Fig. 3

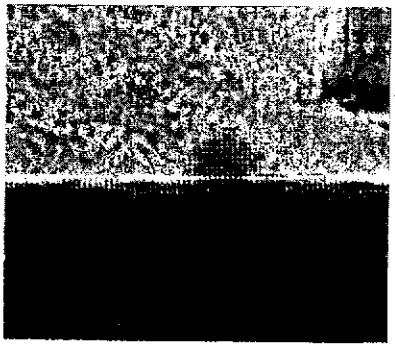

(*a*)

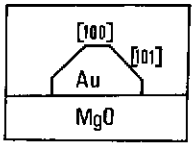

(*b*)

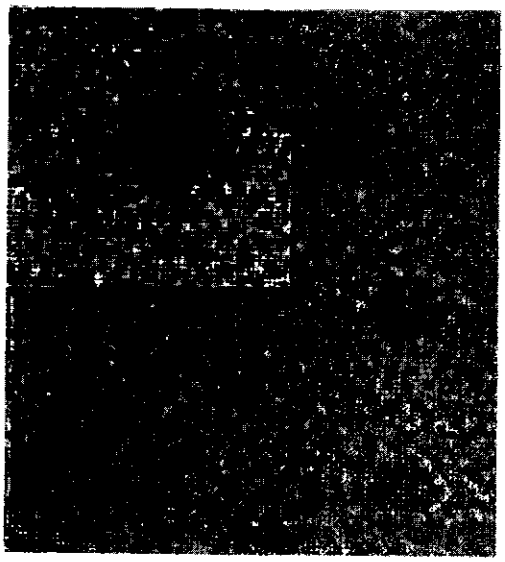

(*c*)

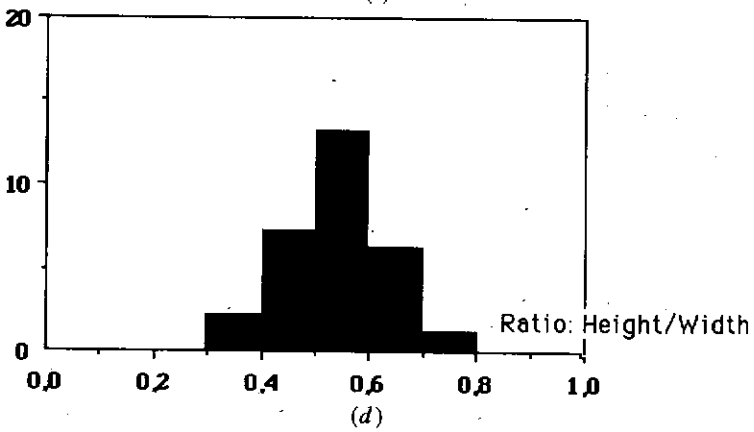

(*d*)

(*a*) High-resolution image in cross-section view of a gold particle on a MgO cube. The 200 and 020 lattice fringes are undistorted at the Au–MgO interface. (*b*) Indexing of the limiting directions of the particle in (*a*). (*c*) High-resolution image of gold particles on the surface of a MgO cube. The particle in the inset belongs to a different MgO cube, but the five particles of the image are at the same magnification. (*d*) Histogram of the ratio of height to width of particles seen in cross-section view (31 particles).

As a consequence, we can say that all the gold particles in the size range 1–4 nm have their lattice perfectly accommodated by the support; therefore the gold lattice parameter is expanded by $2{\cdot}9\% \pm 0{\cdot}5\%$, independently of the particle size. The expansion was seen in the three crystallographic directions by observations of isolated particles in cross-section, both in microdiffraction and in CBED. This expansion was found to be isotropic, to the limits of the errors of the CBED ($\pm 1\%$).

In order to show the difference between the behaviours of large particles, we present some figures from particles larger than 4 nm.

Figure 1 (*c*) represents MgO cubes with particles larger than 4 nm. Using SAD with a beam diameter of 20 nm, diffraction patterns of isolated particles can be obtained. Different epitaxial orientations were found. The diffraction pattern in fig. 2 (*b*) shows a small splitting of the 200 reflections of gold and MgO in the case of (100) epitaxy.

The diffraction pattern in fig. 2 (*c*) shows the 200 reflections of MgO and 220 reflections of gold and MgO. The pattern arises from an isolated particle in the (111) epitaxial orientation on MgO with the relations $(111)_{Au} \| (100)_{MgO}$, $\langle 110 \rangle_{Au} \| \langle 110 \rangle_{MgO}$; however, we can notice a slight azimuthal misorientation. For these large (greater than 4 nm) particles in both (100) and (111) orientations, the measured lattice parameter corresponds to the bulk lattice of gold.

§ 3. HRTEM observations

The samples were imaged with the JEOL 4000 EX microscope at Grenoble, at an accelerating voltage of 400 kV, in order to resolve the atomic structure of the Au–MgO interface. Figure 3 (*a*) shows a profile view of a 3 nm gold particle on the MgO substrate, seen along a $\langle 100 \rangle$ direction. The particle is limited by two $\langle 011 \rangle$ directions, two $\langle 001 \rangle$ directions normal to the interface and one $\langle 001 \rangle$ direction parallel to the interface (fig. 3 (*b*)), which is consistent with a half-octahedron shape with four (111) faces, and truncated at the bottom and at the top by (001) faces. The top view of particles sitting on the MgO (001) surface (fig. 3 (*c*)) clearly shows the four $\langle 110 \rangle$ directions limiting the crystal, and four sides in $\langle 100 \rangle$ directions, indicating the (100) truncations. The extension of the (100) truncations has been evaluated on large particles (greater than 3 nm) by direct measurements of the ratio of the height of a particle to its width at the interface. The histogram is given in fig. 3 (*d*): the average value of $0{\cdot}5 \pm 0{\cdot}1$ indicates roughly equivalent truncations at the edges of the octahedron. The shape of the deposited particles is thus a truncated half-octahedron. Smaller particles with a half-octahedron shape have been imaged (fig. 4) in the same orientation. The exact truncations at the top of the octahedron are not now directly visible in the experimental image. Further results will be published on these smaller particles.

Fig. 4

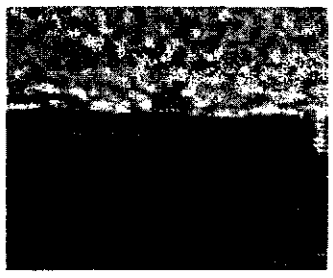

High-resolution image in cross-section view of a 1·2 nm gold particle.

Fig. 5

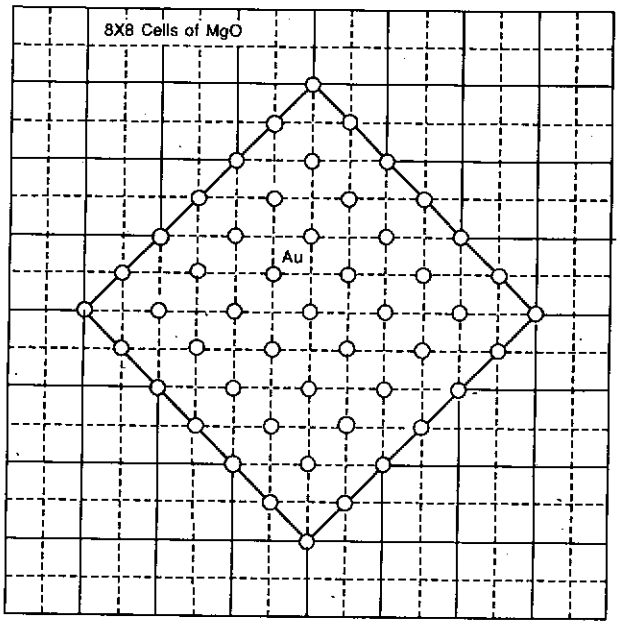

(*a*)

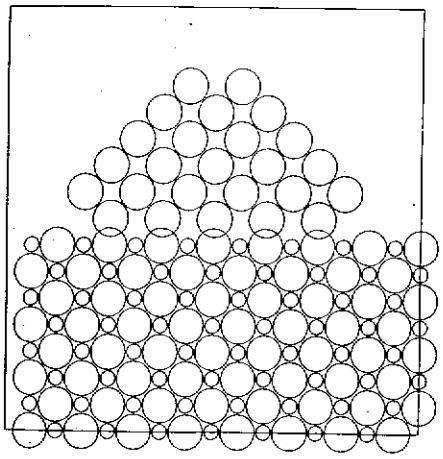

(*b*)

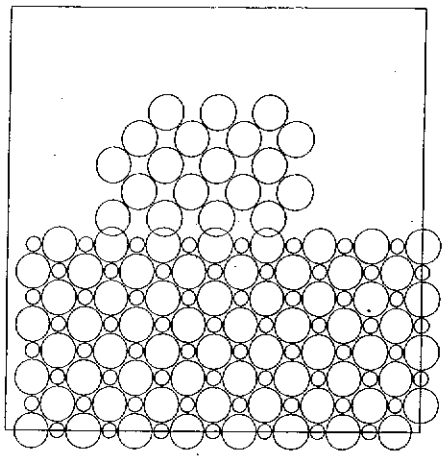

(*c*)

(*a*) Schematic representation in top view of the supercell, taken for the image calculation of the particle. In the calculation, the four atoms of the corners and the isolated atom at the top are omitted. The broken lines represent the (200) planes. The circles represent the centre of the gold atoms in a section of the particle. (*b*), (*c*) Schematic representations in cross-section of the supercell, taken for the image calculation in profile view in figs. 6 (*a*) and (*b*). In this case, gold, magnesium and oxygen are represented individually.

Fig. 6

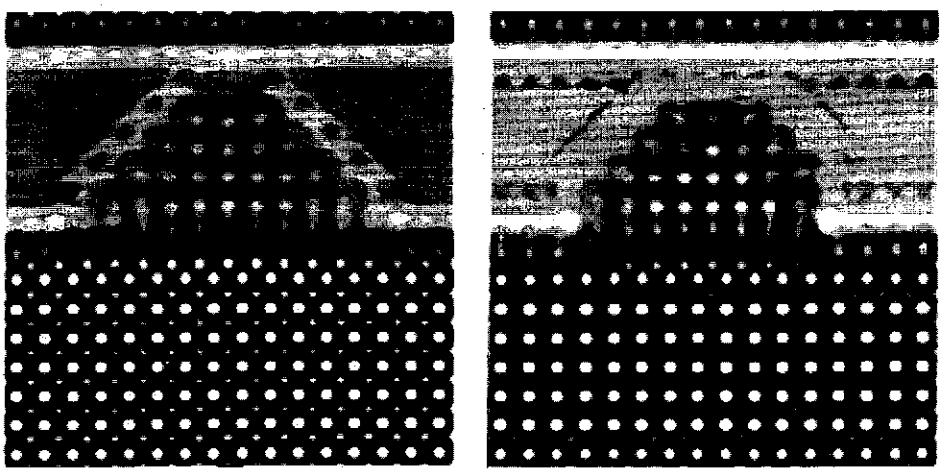

(*a*) (*b*)

Calculated images of gold particles on MgO(001), projected along the ⟨100⟩ direction: (*a*) non-truncated particle; (*b*) particle truncated by a slice of 0·42 nm at the top, 0·42 nm on right-hand side and 0·21 nm on the left-hand side.

Images have been computed by the multislice method, both for a non-truncated and for a truncated half-octahedron of gold, sitting on a MgO surface, the lattice parameter of gold here being equal to that of MgO. For a ⟨100⟩ direction of observation, it was verified that the location of the gold atoms either on the oxygen or on the magnesium atoms does not change the calculated image. A projected supercell of 3·36 nm by 3·36 nm was used (fig. 5). The sampling was done with 256 points along each direction, giving 0·013 nm between two adjacent points; the projected potential was calculated from structure factors corresponding to spatial frequencies up to 37·8 nm^{-1}. No Debye–Waller correction was introduced. Finally, the transfer of the electronic wave through the microscope was described in the usual way, using the parameters of the JEOL 4000 EX microscope (spherical aberration coefficient $C_s = 1{\cdot}05$ nm; beam divergence, 1 mrad; defocus spread, 10 nm). Figures 6 (*a*) and (*b*) show one example for each model, non-truncated or asymmetrically truncated by (100) planes. One can see that the computed and experimental images present similar features. The same calculation was done for a non-truncated half-octahedron of gold sitting on a MgO surface, the lattice parameter of gold now being put equal to the bulk parameter. The small misfit of 2·9% between the particle and the substrate is visible in the simulated image.

§4. Discussion

Gold particles (greater than 1 nm) were condensed on clean surfaces of MgO cubes produced in a controlled atmosphere in the vacuum deposition chamber. For particles smaller than 4 nm, their perfect (001) epitaxial growth was verified by SAD. These particles were found to have a f.c.c. structure with their lattice perfectly accommodated to the MgO substrate. This corresponds to an expansion of the gold lattice parameter of 2·9%. Using CBED on particles in profile view, the expansion of the lattice parameter was measured to be isotropic. For larger (greater than 4 nm) particles, several different orientations were observed by SAD. Their lattice parameter was measured and found

to be equal to that of bulk gold. The variation in the lattice parameter in small gold particles has been measured already by several workers; different techniques have shown a contraction of the parameter for decreasing sizes.

In contrast, in the case of palladium particles, an expansion of the lattice parameter has always been measured (Garmon, Dale and Doering 1983, Heinemann, Osaka and Poppa 1983, Renou and Rudra 1985, De Crescenzi *et al.* 1987, Jacobs and Schryvers 1987, Henry, Chapon, Penisson and Nihoul 1989, Henry and Poppa 1989, Giorgio *et al.* 1990). In our previous experiments on palladium clusters supported on MgO cubes (Giorgio *et al.* 1990), we found a dilatation of the lattice parameter as the particle size decreased, up to 8% for 2 nm particles. At this value of the expansion the two lattices (palladium and MgO) are again perfectly accommodated.

In our preparations of gold epitaxially deposited on MgO, the unexpected dilatation of the lattice parameter, remembering that a contraction has been reported for non-epitaxially oriented particles (Heinemann and Poppa 1985), might be due to the effect of pseudomorphism. Pseudomorphism could also explain our observations on Pd/MgO (Giorgio *et al.* 1990), as well as some results for palladium on graphite (Tardy *et al.* 1991).

Early experiments on the growth (*in situ* in a transmission electron microscope) of gold on MgO(100) showed that (111) epitaxy appears at low temperatures, whereas only the (100) orientation was found at high temperatures (Sato, Shinozaki and Cicotte 1969). The (111) orientation observed at low temperatures was certainly due to the poor vacuum inside the microscope (10^{-4} Pa). Indeed ultra-high-vacuum low-energy electron diffraction experiments on ultra-high vacuum-cleaved MgO have only shown the (100) epitaxy at all temperatures. In contrast, random and then (111) orientations were observed on air-cleaved MgO as the gold coverage was increased (Green, Dancy and Bauer 1970). More recent observations have confirmed the perfect (100) orientation of the gold on MgO (Cowley and Neumann 1984). Pseudomorphism was also observed by HRTEM on the particles profiles on MgO cubes (Marks *et al.* 1988) and also on gold inclusions in the MgO matrix (Tanaka, Nagao and Mihama 1988). The (111) orientation observed for large (greater than 4 nm) particles in fig. 1 (*c*) may be due to partial contamination of the MgO crystal because of the pressure increase during the deposition of these large particles. Further experiments with an improved pumping system are planned.

The HRTEM images of all the particles smaller than 4 nm, observed in plan and in profile views showed single crystals with a half-octahedron shape limited by (111) faces and truncated at the edges by (100) planes. The half-octahedron shape with (100) truncations has already been observed for gold grown *in situ* in a (non-ultra-high-vacuum) electron microscope (Sato *et al.* 1969). This shape has also been observed in our previous investigations on Pd/MgO but in this case we observed a truncation only at the top. Neither structural instability nor coalescence of the particles on MgO was observed during the electron beam irradiation.

At first sight, these observations seem to contradict previous reports on the behaviour of gold particles supported on graphite (Mitome *et al.* 1989), SiO_2 (Iijima 1987) or MgO (Ajayan and Marks 1989), exhibiting structural fluctuations. In fact, as first evidenced by Ajayan and Marks (1989), gold particles epitaxially oriented on MgO are stabilized by the high interfacial energy, preventing quasi-melting. With our preparation conditions, using clean surfaces of prepared MgO microcubes *in-situ*, all the gold particles were perfectly epitaxial leading to pseudomorphism; so that quasi-melting was never observed.

References

Ajayan, P. M., and Marks, L. D., 1988, *Phys. Rev. Lett.*, **60,** 585; 1989, *Ibid.*, **63,** 279.

Balerna, A., Bernieri, E., Picozzi, P., Reale, A., Santucci, S., Burattini, E., and Mobilio, S., 1985, *Surf. Sci.*, **156,** 206.

Cowley, J. M., and Kang, Z. C., 1983, *Ultramicroscopy*, **11,** 131.

Cowley, J. M., and Neumann, K. D., 1984, *Surf. Sci.*, **145,** 301.

De Crescenzi, M., Diociaiuti, M., Lozzi, L., Picozzi, P., and Santucci, S., 1987, *Phys. Rev.* B, **35,** 5997.

Datye, A. K., and Long, N. J., 1988, *Ultramicroscopy*, **25,** 203.

Dundurs, J., Marks, L. D., and Ajayan, P. M., 1988, *Phil. Mag.* A, **57,** 605.

Duriez, C., Chapon, C., Henry, C. R., and Rickard, J. M., 1990, *Surf. Sci.*, **230,** 123.

Garmon. L., Dale, L., and Doering, L., 1983, *Thin Solid Films*, **102,** 141.

Gillet, M., 1977, *Surf. Sci.*, **67,** 139.

Giorgio, S., Henry, C. R., Chapon, C., and Penisson, J. M., 1990, *J. Cryst. Growth*, **100,** 254.

Giorgio, S., Urban, J., and Kunath, W., 1989, *Phil. Mag.* A, **60,** 553.

Green, A. K., Dancy, D., and Bauer, F., 1970, *J. vac. Sci. Technol.*, **7,** 159.

Hall, B. D., Flueli, M., Monot, R., and Borel, J. P., 1989, *Z. Phys*, D, **12,** 97.

Heinemann, K., Osaka, T., and Poppa, H., 1983, *Ultramicroscopy*, **12,** 9.

Heinemann, K., and Poppa, H., 1985, *Surf. Sci.*, **156,** 265.

Henry, C. R., Chapon, C., Penisson, J. M., and Nihoul, G., 1989, *Z. Phys.* D, **12,** 145.

Henry, C. R., and Poppa, H., 1989, *Z. Phys.* D, **12,** 421.

Honjo, G., and Yagi, K., 1980, *Current Topics in Materials Science*, Vol. 6, edited by E. Kaldis. (Berlin: Springer), p. 195.

Howie, A., and Marks, L. D., 1984, *Phil. Mag.* A, **49,** 95.

Iijima, S., 1987, *Microclusters*, Springer Series in Material Sciences, edited by Y. Nishima, S. Onishi and S. Sugano (Berlin: Springer), p. 186.

Ino, S., 1966, *J. phys. Soc. Japan*, **21,** 346; 1969, *Ibid.*, **27,** 941.

Jacobs, J. M., and Schryvers, D., 1987, *J. Catal.*, **103,** 436.

Kern, R., Lelay, G., and Metois, J. J., 1979, *Current Topics in Materials Science*, Vol. 3, edited by E. Kaldis (Berlin: Springer) p. 389.

Kofman, R., Cheyssac, P., and Garrigos, R., 1990, *Phase Transitions*, **24–26,** 283.

Marks, L. D., 1984, *Phil. Mag.* A, **49,** 81.

Marks, L. D., Hong, M. C., Zhang, H., and Teo, B. K., 1988, Materials Research Society Symposium Proceedings, Microstructure and Properties of Catalysis, Vol. III (Pittsburgh, Pennsylvania: Materials Research Society), p. 213.

Marks, L. D., and Smith, D. J., 1983, *J. Microsc.*, **130,** 249.

Mitome, L., Tanishiro, Y., and Takayanagi, K., 1989, *Z. Phys.* D, **12,** 45.

Renou, A., and Rudra, A., 1985, *Surf. Sci.*, **156,** 69.

Sato, H., Shinozaki, S., and Cicotte, L. J., 1969, *J. vac. Sci. Technol.*, **6,** 62.

Tanaka, N., Nagao, M., and Mihama, K., 1988, *Ultramicroscopy*, **25,** 241.

Tanji, T., Masaoka, H., Ito, J., Yada, K., and Cowley, J. M., 1989, *Ultramicroscopy*, **27,** 223.

Tardy, B., Noupa, C., Leclercq, C., Bertolini, J. C., Hoareau, A., Treilleux, M., Faure, J. P., and Nihoul, G., 1991, *J. Catal.* (in press).